A Novel Heuristic Passive and Active Matching Circuit Design Method for Wireless Power Transfer to Moving Objects

Jo Bito (美藤 成), *Student Member, IEEE*, Soyeon Jeong, *Student Member, IEEE*, and Manos M. Tentzeris, *Fellow, IEEE*

***Abstract*— In this paper, a novel matching circuit design method utilizing a genetic algorithm (GA) and the measured S-parameters of randomly moved coil configurations is discussed. Through the detailed comparison of different matching circuit topologies, the superiority of active matching circuits is clearly demonstrated, and potentially there is 21.4% improvement in the wireless power transfer efficiency by using a four-cell active matching circuit, which can create 16 different impedance values. Also, the matching circuit design simulation can be further simplified by choosing a much smaller subset of representative impedance values for the utilized time-changing coil configuration through the employment of *k*-means clustering and use only these values for the derivation of the optimal matching circuit. This heuristic approach could drastically reduce the time for the matching circuit design simulation, especially for matching circuit topologies with a larger number of cells.**

***Index Terms*— Genetic algorithms (GAs), impedance matching, real-time system, wearable, wireless power transfer (WPT).**

I. Introduction

OVER the last decades, wireless power transfer (WPT) technology has attracted a lot of attention from industry and research communities in order to realize highly demanded truly cableless power supply systems. One of the most important applications of this technology is in the medical field, especially for wearable/implantable devices [1]. Also, recently, the demand of wireless charging systems for moving objects, such as electric vehicles [2] and unmanned aerial vehicles (UAVs) [3], has been significantly increased because of the typical short lives of the batteries utilized. There have been several reported types of WPT systems relying on different operation principles. Among them, resonant coupling, especially the magnetic resonant coupling method, utilizing resonating coils, is one of the strongest candidates because of its relatively large maximum operation distance up to a few meters and high maximum power transfer efficiency [4]. This maximum operation range should be long enough to compensate the positioning accuracy next to the charger. However, due to the fundamental operation principle of this method, the WPT efficiency significantly degrades for time-varying transmitter (Tx) and receiver (Rx) coil separation distances, especially the coils are too close with each other. This could be a critical issue for WPT for moving objects such as human bodies and UAVs. In literature, it has been reported that this problem can be solved by utilizing an active matching system even under misaligned conditions in addition to the coil separation distance changes [5], [6].

In previously reported work [6], the main goal was to design an active matching circuit which can be used for different types of coils. To achieve this goal, we tried to design a matching circuit which has an evenly distributing impedance of matching circuit around, where coil-coupling is high and therefore WPT efficiency is potentially high. However, with this design goal, the active matching circuit ended up using 6 cells whose nonideal lumped components caused inevitable losses and discrepancies between modeled and effective impedance values. Also, the matching circuit combination selection time, while operating the active matching system utilizing brute force selecting, is relatively long. However, in more realistic situations, the impedance of the Tx–Rx coil network continuously changes because of the coils movements, and the reconfigurability speed of the utilized matching network needs to be drastically improved. In the previous conference paper, a novel matching circuit design method utilizing the combination of a genetic algorithm (GA) with clustering, which can maximize the performance of both fixed-value passive matching circuits or active matching circuits that are composed of a combination of inductors, capacitors, and p-i-n diodes, was analytically discussed. This method was based on the measured coil configuration S-parameters under real-time moving conditions, which displayed tendencies/unven space distribution in the coil impedance values. This was used to minimize the number of cells in the active matching circuit, which eventually reduced the brute force matching circuit selection process while the system was operating [7]. As depicted in Fig. 1, the designed matching circuits are connected between the signal source and the Tx coil. In this paper, the matching circuit design accuracy has been further enhanced by introducing the measured S-parameters of the utilized lumped components, and the performance of the designed matching circuit is validated through the comparison between the simulations and the experiments. Also, this paper discusses the

Manuscript received July 22, 2016; revised January 17, 2017 and February 6, 2017; accepted February 12, 2017. Date of publication March 15, 2017; date of current version April 3, 2017. This work was supported in part by the National Science Foundation and in part by Defense Threat Reduction Agency. This paper was presented at the IEEE MTT-S Wireless Power Transfer Conference, Aveiro, Portugal, May 5–6, 2016.

The authors are with the School of Electrical and Computer Engineering, Georgia Institute of Technology, Atlanta, GA 30332-250 USA (e-mail: jbito3@gatech.edu).

Color versions of one or more of the figures in this paper are available online at http://ieeexplore.ieee.org.

Digital Object Identifier 10.1109/TMTT.2017.2672544

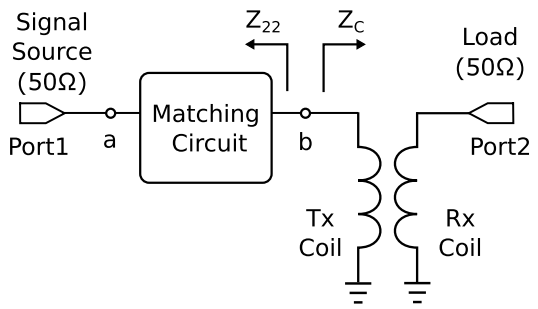

Fig. 1. Block diagram of the WPT system with the optimized matching circuit in the Tx side.

bias circuit design for the active matching circuit to minimize the discrepancy in impedance value while RF input power is high.

II. Characterization of Tx–Rx Coil Impedance Under Moving Condition

In order to characterize the effect of the movements of the Tx–Rx coils on the coil input impedance for a proof-of-concept topology, the S-parameters of the Tx–Rx topology were periodically measured using a vector network analyzer (VNA), ZVA8 from Rohde & Schwarz, which was controlled by using LabVIEW. Without loss of generality, 10-cm-diameter open helical coils with the resonance frequency of 13.6 MHz were used as both Tx and Rx coils. The S-parameters of the time-changing Tx–Rx topologies were measured 100 times with the time interval of 250 ms by randomly changing the distance and the elevation without rotating the coil within the coils for center-to-center coil distances in the range of about 10–20 cm. The coil orientation change associated with the rotation of the coils typically changes the mutual inductance between two coils. Therefore, similar change in impedance value while changing the separation distance may happen because of the coil rotation. However, rotating the coil adds more complexity in measurement and it was difficult to rotate the coil without the effects of a mechanical coil holder to the electrical property of the coils. Thus, this research did not consider the rotation of the coil. During the measurements, the coils were placed on sponges, avoiding their interaction with hands, and manually moved. The same experiment was repeated four times, and the measured Tx–Rx coil topology input impedance (Z_c) values for all trial measurements are shown in Fig. 2. As it can be easily observed, Z_c varies in a quite wide range, but there is a clear tendency/space concentration in the distribution of the coil impedance values. In Fig. 3, the distribution of power transfer efficiency, $|S_{21}|\times 100$ (%), of the above described 400 (4×100) measurements along with their arithmetic mean are depicted. The average power transfer efficiency without any matching circuit is about 60.8 % [7].

III. Matching Circuit Design Using GA

GAs are heuristic searching methods, which can be applied to many engineering problems. This approach is especially suitable to solve the problems that could require a variety of

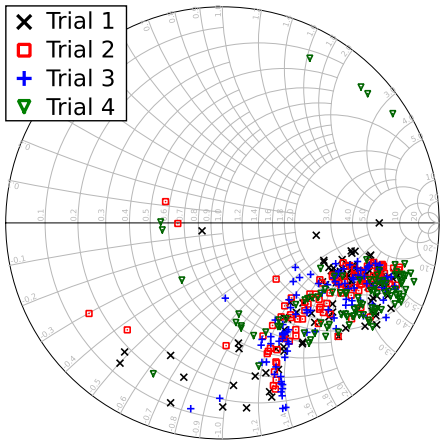

Fig. 2. Measured input impedances of Tx–Rx coil topology under random coil movements in four trials of 100 measurements each.

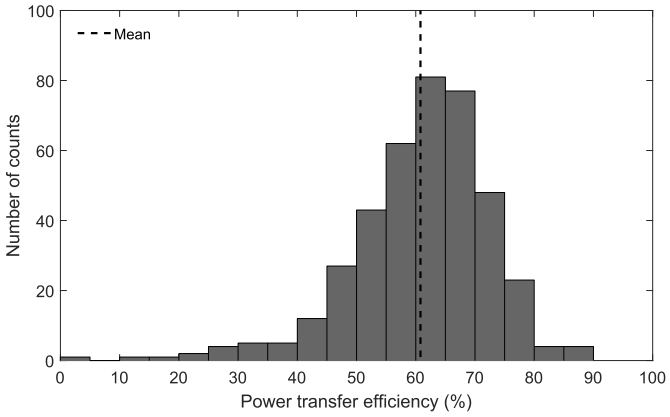

Fig. 3. Distribution and arithmetic mean of the measured power transfer efficiency values for four trials with 100 measurements each (total of 400 counts).

discrete values as potential solutions. For the easy and quick implementation of the GA, MATLAB Global Optimization Toolbox was utilized. For this research, first, the fixed-value passive matching circuit topology is discussed and evaluated in terms of the optimization of the power transfer efficiency to moving coils. Next, the GA-based matching circuit design process is extended to active matching circuit designs.

In general, a cascaded two-port network/topology can be modeled through the multiplication of the respective stage transmission (*ABCD*) matrices. The *ABCD* matrix of each trial measurement (sample) can be obtained from the measured S-parameters of the corresponding Tx–Rx coil network by converting the S-matrix to the *ABCD* matrix. Once the *ABCD* matrix of the matching circuit is determined by choosing the values of its lumped components, the S-matrix of the cascade of the matching circuit and the Tx–Rx coils topology can be computed from the total transmission matrix [8]. Assuming that there are M samples of S-parameters for the time-changing coil configurations, the probability of choosing the ith sample (P_i) is $1/M$. In the presented approach, the power transfer efficiency (η) is defined as the expected value of $|S_{21}|$ for the composite matching+coil configuration, as described in (1). For active matching circuits that feature more than

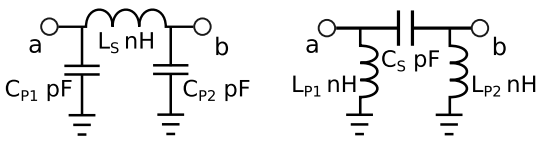

Fig. 4. Pi matching circuit topologies with a series inductor (left) and a series capacitor (right).

TABLE I

CIRCUIT COMPONENT VALUES FOR OPTIMIZED FIXED PI MATCHING CIRCUIT TOPOLOGIES USING IDEAL LUMPED COMPONENT MODELS

Ser L		Ser C	
L_S	1000 nH	C_S	10.0 pF
C_{P1}	0 pF	L_{P1}	1000 nH
C_{P2}	39 pF	L_{P2}	720 nH

two potential matching circuit configurations, the maximum $|S_{21}|$ value among all possible $|S_{21}|$ values for the ith sample topology is chosen. The fitting function for the GA simulation is defined as F in (1), and the matching circuit component values, which can minimize the value of F have to be identified and selected

$$F = 100 - \eta, \quad \text{where } \eta = \sum_{i=1}^{M} |S_{21}|^i_{\text{Max}} \; P_i \times 100 \; (\%). \quad (1)$$

A. Fixed-Value Passive Matching Circuit

In order to determine the optimal fixed-value passive matching circuit topology, two Pi matching circuits, one featuring a series inductor with two parallel capacitors (Ser L), and another one featuring a series capacitor with two parallel inductors (Ser C) are defined. The two Pi matching circuits are depicted in Fig. 4. For the sake of practicality, for both inductors and capacitors, 29 consecutive commonly used circuit values (10–2000 nH for inductor and 10–2000 pF for capacitor), which cover a lumped element value range of more than 100:1 for the operation frequency of 13.6 MHz were considered. The range of lumped component values were chosen after less than ten times of iterations of GA simulations, confirming the values out of this range have never been used. Lumped component values below this range do not make sufficient change in impedance value, and the values above potentially cause too much change in impedance value as a single step. Also, the parallel components are allowed to be placed in an "open circuit" position, which can virtually lead to L-type matching circuits. The "ideal" circuit component values that minimize the fitness function for each fixed-value Pi-matching circuit topology are shown in Table I.

B. Active Matching Circuit

For proof-of-concept demonstration purposes, in this paper, a discrete value impedance matching circuit including p-i-n diode switches is adopted because of its fast switching speed, miniaturized size, and robustness [8]. The matching circuit topology is based on the N-stage cascading of a unit cell

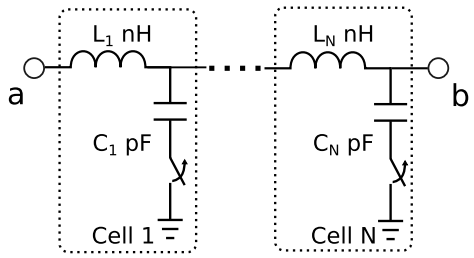

Fig. 5. N-stage active matching circuit schematic.

TABLE II

CIRCUIT COMPONENT VALUES FOR OPTIMIZED ACTIVE MATCHING CIRCUITS WITH DIFFERENT NUMBER OF CELLS USING IDEAL LUMPED COMPONENT MODELS

	Inductors (nH)				Capacitors (pF)			
	L_1	L_2	L_3	L_4	C_1	C_2	C_3	C_4
cell (1C)	1000	-	-	-	47	-	-	-
cell (2C)	330	820	-	-	390	47	-	-
cell (3C)	330	330	820	-	150	330	39	-
cell (4C)	330	470	0	820	180	330	82	33

TABLE III

FIGURE OF MERIT OF EACH MATCHING CIRCUIT TOPOLOGY

	No MC	Ser L	Ser C	1 C	2 C	3 C	4 C
Efficiency (%)	61.5	76.4	76.4	78.3	80.8	82.2	82.9
Improvement (%)	-	14.9	14.9	16.8	19.3	20.7	21.4
Error (%)	-	15	13	10	4	1	1

consisting of an L-type unit cell comprising of a series inductor, a shunt capacitor, and a switch as shown in Fig. 5. Without loss of generality and to facilitate the fabrication, the additional dc blocking capacitors have not been included in the preliminary design process discussed in this section. Their concurrent optimization will be described in Section VI. The utilized N stages can create 2^N different impedance values. For both inductors and capacitors, 29 consecutive component values were used, which are the same as those in the case of the fixed-value passive matching circuits. In this case, the inductance values are allowed to be 0 ("short circuit"). The circuit component values, which minimize the fitness function for 1 (1C)-4 (4C) utilized stages/cells are shown in Table II.

In Table III, the figure of merit (power transfer efficiency) for each optimized matching circuit topology is summarized. The improvement is obvious in the significant difference of the power transfer efficiency value compared with the case of no matching circuit (No MC). The "error" represents the number of data points where the power efficiency is lower than that for the case of no matching circuit within the 100 samples in Trial1. As Table III clearly displays, the active matching circuit is much more efficient in improving the power transfer efficiency compared with the passive fixed-value matching circuit. As the number of the stages/cells increases, the efficiency increases while simultaneously reducing the "error" rate. From this simulation, it can be deduced that three cells or four cells are sufficient to optimally improve the power transfer efficiency as the improvement saturates for

TABLE IV

POWER TRANSFER EFFICIENCY COMPARISON USING MEASURED S-PARAMETERS FOR TRIALS 1–4

	No MC	Ser L	Ser C	1 C	2 C	3 C	4 C
Efficiency (Trial1) (%)	61.5	76.4	76.4	78.2	80.8	82.2	82.9
Efficiency (Trial2) (%)	60.1	73.6	73.6	75.4	76.8	78.1	78.5
Efficiency (Trial3) (%)	59.9	72.8	72.9	75.4	77.4	78.3	79.2
Efficiency (Trial4) (%)	61.6	79.2	79.1	80.6	82.9	85.6	86.2
Degradation (%)	-	2.0	1.9	1.4	2.6	2.7	2.9

larger number of stages, where an efficiency of 78.3-82.9% is achieved. As a comparison, the power transfer efficiency using the previously designed six cell active matching circuit is 72.2 % [6]. This implies that a higher power transfer efficiency can be achieved even with a significantly smaller number of cells compared with previously reported matching circuits. Although, the matching circuits reported in the previous papers were designed to improve the power transfer efficiency of different generic types of coils, the matching circuits introduced in this paper can be easily customized and optimized for specific coil configurations. This design approach difference is one of the main causes for enhanced power transfer efficiency.

In order to confirm whether the designed matching circuits that are based on the measured data (100 measurements) of Trial1 can also work for other sets of sampled data, the power transfer efficiencies for each trial is computed and summarized in Table IV. It can be easily observed that there is no significant performance degradation of the data for different trials.

IV. k-MEANS CLUSTERING

Since there is a clear trend in the distribution of coil impedance values over the Smith chart, it is possible to drastically reduce the time for GA simulation by selecting only representative impedance values as targets instead of using all sampled/measured data. Also, the fitness function calculation, which includes numerous S-to-*ABCD* matrix conversions, is not very computationally efficient. In order to choose a much smaller but almost equally efficient subset of coil configuration impedance values, we employed the k-means clustering method, which is commonly used for the data mining from big data, utilizing MATLAB. In the k-means clustering method, the program selects an arbitrary positive integer (K) of clusters, which are the subsets of data points by minimizing the function C expressed in (2). In (2), $d(x, g_i)$ is the distance between each data point (x) in ith cluster (S_i), and the centroid of ith cluster (g_i). At the beginning of the data mining, we have automatically generated 100 replicates as starting points of the clustering in order to increase the accuracy of the clustering [9], [10]. In this case, replicates are 100 complex numbers whose upper and lower boundary values are determined from the measured coil configuration impedance values (Z_c) in Trial 1. The values of replicates are automatically selected minimizing the sum of distances between each replicate in the complex plane. For the proof-of-concept demonstration of the implementation of the clustering data mining method, 4, 8, and 16 representative coil topology

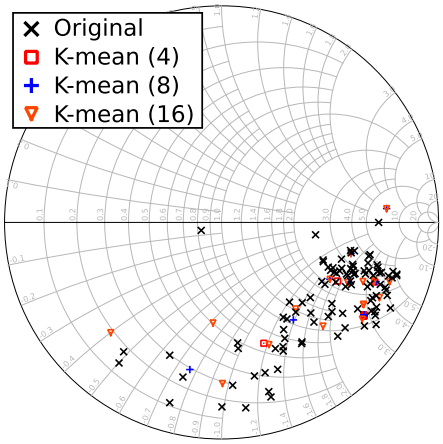

Fig. 6. Measured 100 input impedance values of Tx–Rx coils configurations under random movements in Trial1 and representative impedance values selected by using k-means clustering.

TABLE V

POWER TRANSFER EFFICIENCY COMPARISON BETWEEN ALL 100 MEASURED DATA VERSUS 4, 8, AND 16 CLUSTER REPRESENTATIVE IMPEDANCE VALUES

	No MC	Ser L	Ser C	1 C	2 C	3 C	4 C
Efficiency (100) (%)	61.5	76.4	76.4	78.3	80.8	82.2	82.9
Efficiency (K-4) (%)	-	35.5	75.2	78.3	79.6	81.6	82.0
Efficiency (K-8) (%)	-	62.6	76.0	78.0	79.5	81.7	82.5
Efficiency (K-16) (%)	-	62.6	75.8	77.6	79.5	81.6	82.3

input impedance values are chosen by using the 100 measured S_{11} values in Trial 1. In Fig. 6, the Trial 1's 100 sampled impedance values are plotted along with 4 (K-4), 8 (K-8), and 16 (K-16) clustered impedance values

$$C = \sum_{i=1}^{K} \sum_{x \in S_i} (d(x, g_i))^2. \tag{2}$$

Since the power transfer to the load can be maximized when the input impedance of the matching circuit looking from port 2 (Z_{22}) in Fig. 1 is the complex conjugate of the Tx–Rx coil topology impedance input (Z_C), the sum of the reflection coefficient between the ith clustered (coil topology) impedance value and Z_{22} is introduced as a new fitness function (G) as described in (3). In (3), Z^*_{Ci} is the complex conjugate of the imaginary part of Z_C, and $|\Gamma|^i$ is the reflection coefficient for the ith sample. Since active matching circuits have more than two potential matching circuit configurations, the minimum reflection coefficient among all potential matching circuit states ($|\Gamma|^i$) was chosen

$$G = \sum_{i=1}^{L} |\Gamma|^i_{\mathrm{Min}}, \quad \text{where } \Gamma = \frac{Z^*_{\mathrm{Ci}} - Z_{22}}{Z^*_{\mathrm{Ci}} + Z_{22}}. \tag{3}$$

In Table V, the power transfer efficiency values for the matching circuit topologies optimized using only the clustered data (4, 8, and 16 points) as the target impedances in the GA simulation is summarized. From Table V, it can be easily concluded that there are some cases that the clustered data do not work as proper targets, especially for the series inductor

TABLE VI

CIRCUIT COMPONENT VALUES FOR OPTIMIZED FIXED PI MATCHING CIRCUIT TOPOLOGIES USING NONIDEAL LUMPED COMPONENT S-PARAMETERS MODELS

Series L		Series C	
L_S	1000 nH	C_S	120 pF
C_{P1}	12 pF	L_{P1}	1800 nH
C_{P2}	39 pF	L_{P2}	820 nH

TABLE VII

CIRCUIT COMPONENT VALUES FOR OPTIMIZED ACTIVE MATCHING CIRCUITS WITH DIFFERENT NUMBER OF CELLS USING NONIDEAL LUMPED COMPONENT S-PARAMETERS MODELS

	Inductors (nH)				Capacitors (pF)			
	L_1	L_2	L_3	L_4	C_1	C_2	C_3	C_4
1 cell	1000	-	-	-	47	-	-	-
2 cell	820	820	-	-	270	56	-	-
3 cell	560	4.3	820	-	100	330	33	-
4 cell	560	4.3	820	5.6	100	330	39	22

Pi matching circuit case, and degrade the performance of matching as the cluster size decreases. However, in most cases (series C passive and one- to four-stage active matching circuits), the clustering of impedance values does not have a significant effect on the matching circuit design performance.

V. MATCHING CIRCUIT DESIGN USING NONIDEAL LUMPED COMPONENT MODELS

In order to further increase the accuracy of the matching circuit design using genetic optimization algorithms, the measured S-parameters data for each nonideal utilized lumped element provided by the vendors are introduced in MATLAB simulations. Each matching circuit component was replaced by its two-port S-parameters model, and the impedance of the entire matching circuit network was represented as a cascade of *ABCD* matrices derived from the S-parameters. For a proof-of-concept simulation, the utilized series inductor and parallel capacitor in the L-shape matching unit cells of Fig. 5 are Coilcraft 0603CS and 0603HL, and Taiyo Yuden UMK105CG series, respectively. For this simulation, 55 inductor values (1.6–1800 nH) and 29 capacitor values (12–1000 pF) in the design kits were used. The circuit component values, which are used for the final design of every matching circuit topology are summarized in Tables VI and VII. There are slight changes in the optimized component values compared with Tables II and III due to the parastics of the nonideal lumped components compared with the original capacitance and inductance values in the ideal matching circuits. The performance of the matching circuits using nonideal lumped component models is discussed in Section VII.

VI. DC BIAS CIRCUIT DESIGN

In previously reported results, it has been confirmed that the RF isolation of dc bias circuits in the active matching configurations has not been good enough and has typically led to slight shifts in the impedance values of the matching

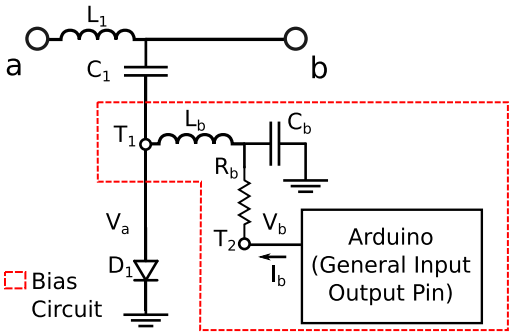

Fig. 7. Circuit topology of the active matching circuit unit cell including the switch-controlled dc bias circuit.

circuits as to an increased dissipative loss. Therefore, the dc bias circuits of the p-i-n diode switches, which are typically composed of a series inductor (L_b), a parallel capacitor (C_b) and a current limiting resistance (R_b), as depicted in Fig. 7, are also optimized in our proposed approach by changing the values of the lumped components to reduce the undesired impedance value shift and dissipative loss. The S_{11} and S_{21} of both the original (initial design before optimization) and the optimized bias circuits are depicted in Fig. 8(a) and (b), respectively assuming that the port1 is T_1 and the port2 is T_2 in Fig. 7 and both are connected to 50 Ω [11]. From Fig. 8(a), it can be easily observed that the return loss of the original bias circuit is not as high as for the optimized circuit, thus being one of the main causes of undesired impedance value shifts. For the new design, a 100 μH inductor, DLW43SH101 from Murata, which provides the highest series inductance satisfying the self-resonant frequency above 13.6 MHz, was used.

Due to the main operation principle of previously reported real-time matching systems, the switching speed must be faster than the reading of analog to digital converter (ADC) virtually controlling the switching status [6]. In the presented proof-of-concept prototype, an Arduino Uno micro-controller unit was used for the control of the p-i-n diode switches of the active matching circuit stages. From its datasheet, the sampling speed of Arduino is 9.6 ks/s, which implies that the response time of the diode switch must be below 100 μs. The value of C_b was chosen to be the highest capacitance value that satisfies the limitation of 100 μs LC response time for further RF isolation as can be seen in Fig. 8(a) and (b). In Fig. 8(c), the transient of the diode anode voltage (V_a) is depicted. The response time can be improved by removing C_b without a significant effect on RF isolation, and this can be an option when a micro-controller chip which features the capability of faster ADS reading, for example MSP432 (200 ks/s), is used.

From the datasheet, Arduino module has a rated output current of 20 mA with 5 V output voltage, and the value for R_b needs to be adjusted to satisfy this condition. The simulation results of the bias current (I_b) for an input power level of 30 dBm and bias voltage is 5 V is shown in Fig. 8(d), and it turns out that the resistance in the original design is too high and the resulting current is unstable. R_b can be further lowered to 200 Ω for further stabilization. The original and

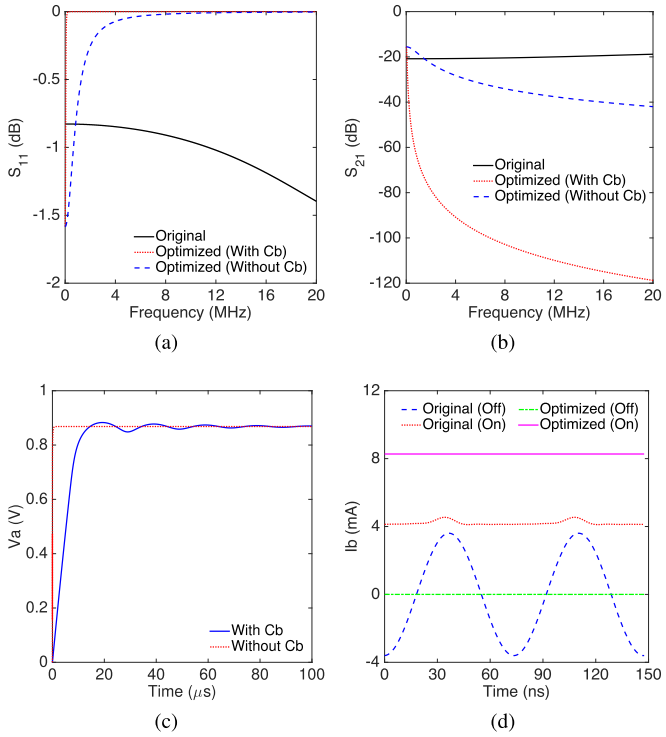

Fig. 8. (a) S_{11} of the original and of the optimized bias circuits. (b) S_{21} of the original and of the optimized bias circuits. (c) Transient of the diode anode voltage after switching. (d) Steady-state bias current at ON/OFF states for the original and the optimized bias circuit.

TABLE VIII
PARAMETERS OF ACTIVE MATCHING CIRCUIT UNIT CELL DC BIAS COMPONENTS

	L_b	C_b	R_b
Original	330 nH	82 pF	1 kΩ
Optimized	100 μH	0.1 μF	500 Ω

the optimized value of each circuit component are summarized in Table VIII.

VII. MEASUREMENT RESULTS AND DISCUSSION

A. Active Matching Circuit Operation Tests

Based on the optimized active matching circuit design using GA on MATLAB, the prototype of an 1-cell active matching circuit was fabricated as shown in Fig. 9. The series inductor and the parallel capacitor in the L-matching unit cell network, shown in Fig. 7, are Coilcraft 0603HL and Taiyo Yuden UMK105CG series, respectively. Also, the p-i-n diode is Skyworks SMP1340.

The two-port S-parameters of the 1-cell matching circuit at "ON" and "OFF" states were measured using the VNA for an input power level of 0 dBm at 13.6 MHz and the S_{11} measured values for both states are plotted in Fig. 10. The bias voltage at "ON" condition is 5 V from Arduino Uno module. For comparison purposes, ADS simulation results for the same matching circuit topology with ideal components ("Ideal") and nonideal components utilizing their respective S-parameters ("S-parameter") are also depicted in the

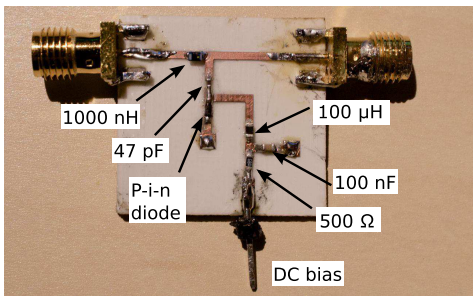

Fig. 9. Prototype of an one-cell active matching circuit.

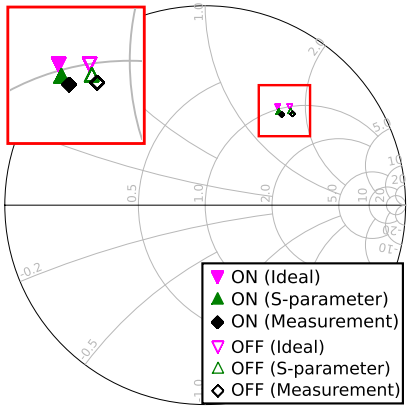

Fig. 10. Measured and simulated input impedances of one-cell active matching circuit at ON and OFF conditions.

same figure. As it can be easily observed from Fig. 10, there are slight differences between the simulation results with ideal components and the measurement results. The simulation results using the nonideal components' S-parameters and the nonideal diode model are closer to the measurement results, which implies that GA matching design process can be improved by integrating S-parameters of each lumped component instead of using ideal values.

The S_{11} values of the matching circuit at "ON" and "OFF" states were also measured for different input power levels. The output power from the VNA was calibrated using the power sensor, NRP-Z211 from Rohde & Schwarz, at 15 dBm which is the maximum output power from the VNA at 13.6 MHz. The measurement results for the input power levels of 15, 0, and −10 dBm are depicted in Fig. 11(a) and (b). It can be easily recognized from Fig. 11(a) and (b) that there are slight differences in the input impedance values in the case of the input power level of 15 dBm compared with the other input power levels, but these differences are very small and can be omitted throughout the whole input power level range; this difference can increase for higher power levels (that are closer to the rated power of 250 mW for the SMP1340 p-i-n diode). For more practical applications, such as the charging of electric vehicle and UAVs, which require a power handling capability that is typically more than 250 mW, p-i-n diodes or other switching elements such as mechanical arrays, which have higher rated power, should be used. Even if different switching elements are used, the proposed matching circuit design method can be

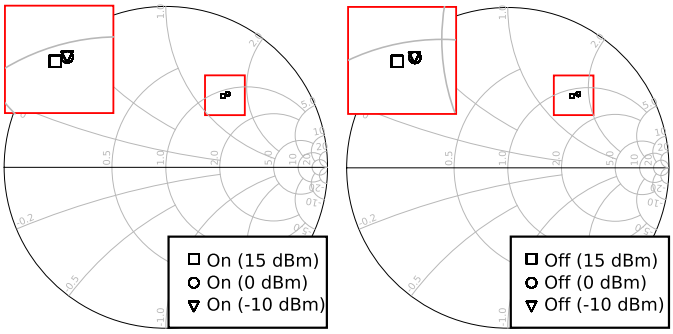

Fig. 11. Measured input impedance of the one-cell active matching circuit for different input power levels at (a) "ON" and (b) "OFF" switch conditions.

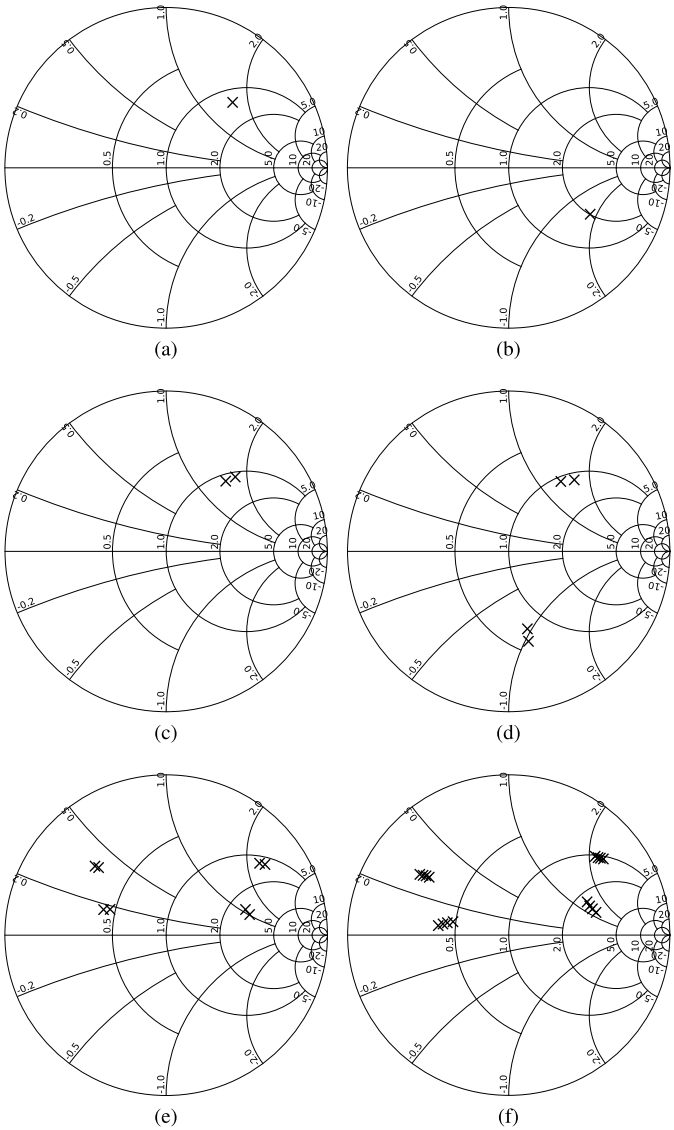

Fig. 12. Measured input impedance of (a) L- and (b) C-series passive (c) one-cell, (d) two-cell, (e) three-cell, and (f) four-cell matching circuit.

applied as long as the characteristics of the switching elements are close enough to that of an ideal switch.

TABLE IX

POWER TRANSFER EFFICIENCY COMPARISON WITH EACH MATCHING CIRCUIT WITH IDEAL LUMPED COMPONENTS, NONIDEAL S-PARAMETERS MODELS, AND MEASURED S-PARAMETERS

	No MC	Ser L	Ser C	1 C	2 C	3 C	4 C
Efficiency (Ideal) (%)		76.4	76.4	78.2	80.8	82.2	82.9
Efficiency (Non-ideal) (%)	61.5	73.2	70.7	75.1	76.3	77.4	77.9
Efficiency (Measurement) (%)		72.3	61.7	73.8	75.2	72.8	73.1

B. Passive and Active Matching Circuits Performance Comparison

In addition to the 1-cell active matching circuit, five other matching circuit topologies were also fabricated based on the simulation results shown in Table VI and Table VII. The measured input impedance of each matching circuit at all possible switching conditions are depicted in the Smith charts in Fig. 12. The bias circuit design is the same for all active matching circuits. At the end, the power transfer efficiency for the six fabricated matching prototypes when connected to the Tx–Rx coil configurations described by the 100 samples of Trial1 was calculated using equation (1). The results for the implementations with ideal lumped circuit models, nonideal lumped component S-parameter models and measured S-parameters are summarized in Table IX. From the table, it can be easily concluded that the measurement results are matching well with the simulation results in the cases of the passive matching circuit, and of the 1- and 2-cell active matching circuits. However, as the number of the stages/cells increases, the improvement of the measured power transfer efficiency saturates faster than the simulations, an effect that can be attributed to the increased dissipative loss associated with the increased number of nonideal lumped components and p-i-n diodes in the circuit.

C. Discussion for Practical Applications

For more practical applications, ideally, it is better to use an active matching circuit which has a very wide variety of impedance values and then downselect the optimal impedance combinations for different coil combinations using a GA or a machine learning process as discussed in [12]. However, typically "off-the-shelf" trimmable capacitor ICs similar to the one used in [7] have a relatively low power handling capability and cannot be used for high power applications. Therefore, the proposed method requires the preliminary measurements of coil impedance to decide the combination of lumped components in the matching circuit which cannot be changed after the fabrication. Thus, one of the practical approaches is to standardize the coil design and make a library of measured impedance values for different coil combinations to avoid the repetitive coil impedance measurements. Also, for the charging of actual moving objects, the adjustment of time interval between each brute force matching circuit combination selection depending on the speed of the moving object to maximize the performance of the active matching may be required. Furthermore, the transition of the coil impedance value while the object is moving is expected to have a tendency depending on the type of movement. Therefore, some active

learning process and the real-time prediction of coil impedance value can be introduced in the system to further improve the performance of the matching circuit combination selection process rather than a simple repetitive brute force selection method.

VIII. Conclusion

In this paper, a novel matching circuit design method utilizing a combination of a GA with a data clustering approach based on the measured S-parameters of randomly moving coils was introduced. From the analytical comparison of different matching circuit topologies, the superiority of active matching circuits is confirmed, and potentially there is a 21.4 % improvement in the WPT efficiency by using a four-cell active matching circuit. Also, the matching circuit design simulation can be further simplified by choosing only a subset of representative impedance values as targets utilizing k-means clustering. The matching circuit design time can be reduced to less than 20 min from 2–7 h for arbitrary coil shapes and the new fitting function without a significant effect on the matching circuit performance. Various measurements of a 1-cell active matching circuit input impedance have been demonstrated, and it is suggested that it is possible to further improve the accuracy of the matching circuit design by integrating the S-parameters of each "off-the-shelf" lumped component in the matching design process in order to accurately account for nonideal parastics. Finally, the measurement results have shown a very close agreement with the simulations, and the experimental improvement in power transfer efficiency up to 13.7 % was confirmed for active matching circuit prototypes.

References

[1] A. K. R. Rakhyani, S. Mirabbasi, and M. Chiao, "Design and optimization of resonance-based efficient wireless power delivery systems for biomedical implants," *IEEE Trans. Biomed. Circuits Syst.*, vol. 5, no. 1, pp. 48–63, Feb. 2011.

[2] J. Shin *et al.*, "Design and implementation of shaped magnetic-resonance-based wireless power transfer system for roadway-powered moving electric vehicles," *IEEE Trans. Ind. Electron.*, vol. 61, no. 3, pp. 1179–1192, Mar. 2014.

[3] C. Song *et al.*, "Three-phase magnetic field design for low EMI and EMF automated resonant wireless power transfer charger for UAV," in *Proc. IEEE Wireless Power Transf. Conf.*, May 2015, pp. 1–4.

[4] H. Shoki, "Issues and initiatives for practical deployment of wireless power transfer technologies in Japan," *Proc. IEEE*, vol. 101, no. 6, pp. 1312–1320, Jun. 2013.

[5] T. C. Beh, M. Kato, T. Imura, S. Oh, and Y. Hori, "Automated impedance matching system for robust wireless power transfer via magnetic resonance coupling," *IEEE Trans. Ind. Electron.*, vol. 60, no. 9, pp. 3689–3698, Sep. 2013.

[6] J. Bito, S. Jeong, and M. M. Tentzeris, "A real-time electrically controlled active matching circuit utilizing genetic algorithms for wireless power transfer to biomedical implants," *IEEE Trans. Microw. Theory Techn.*, vol. 64, no. 2, pp. 365–374, Feb. 2016.

[7] J. Bito, S. Jeong, and M. M. Tentzeris, "Heuristic passive and active matching circuit design method for wireless power transfer for moving objects," in *Proc. IEEE Wireless Power Transf. Conf.*, Aveiro, Portugal, May 2016, pp. 1–4.

[8] C. Sanchez-Perez, J. de Mingo, P. L. Carro, and P. Garcia-Ducar, "Design and applications of a 300–800 MHz tunable matching network," *IEEE J. Emerg. Sel. Topics Circuits Syst.*, vol. 3, no. 4, pp. 531–540, Dec. 2013.

[9] D. Arthur and S. Vassilvitskii, "k-means++: The advantages of careful seeding," in *Proc. 18th Annu. ACM-SIAM Symp. Discrete Algorithms*, 2007, pp. 1027–1035.

[10] S. Lloyd, "Least squares quantization in PCM," *IEEE Trans. Inf. Theory*, vol. MTT-28, no. 2, pp. 129–137, Mar. 1982.

[11] J. Bito and M. M. Tentzeris, "Bias circuit design for a real-time electrically controlled active matching circuit utilizing p-i-n diode switches for wireless power transfer," in *Proc. IEEE Antennas Propag. Soc. Int. Symp.*, Fajardo, Puerto Rico, USA, Jun./Jul. 2016, pp. 405–406.

[12] J. Bito, M. M. Tentzeris, and A. Georgiadis, "A hybrid heuristic design technique for real-time matching optimization for wearable near-field ambient RF energy harvesters," in *IEEE MTT-S Int. Microw. Symp. Dig.*, May 2016, pp. 1–4.

Jo Bito (S'13) received the B.S. degree in electrical and electronic engineering from Okayama University, Okayama, Japan, in 2013, and the M.S. degree in electrical and computer engineering from the Georgia Institute of Technology, Atlanta, GA, USA, in 2016, where he is currently pursuing the Ph.D. degree.

From 2010 to 2011, he joined the International Programs in Engineering at the University of Illinois at Urbana–Champaign, Champaign, IL, USA. He is currently a Research Assistant with the Agile Technologies for High-Performance Electromagnetic Novel Applications Group, Georgia Institute of Technology. His current research interests include the application of inkjet printing technology for flexible and wearable electronics, RF energy harvesting, and wireless power transfer systems.

Mr. Bito was a recipient of the Japan Student Services Organization Long Term Scholarship in 2013.

Soyeon Jeong (S'14) was born in Seoul, South Korea. She received the B.E. degree in electrical engineering from Gangneung-Wonju National University, Gangneung, South Korea, in 2010, and the M.E. degree in electrical and computer engineering from the Georgia Institute of Technology, Atlanta, GA, USA, in 2014, where she is currently pursuing the Ph.D. degree at the Agile Technologies for High-Performance Electromagnetic Novel Applications Group, under the supervision of Dr. M. M. Tentzeris.

Her current research interests include wireless power transfer on methods, sensor component design, high-frequency characterization and environmental testing to the design, and the simulation and fabrication of the RF system embedding the sensor.

Manos M. Tentzeris (S'89–M'92–SM'03–F'10) received the Diploma (*magna cum laude*) in electrical and computer engineering from the National Technical University of Athens, Athens, Greece, and the M.S. and Ph.D. degrees in electrical engineering and computer science from the University of Michigan, Ann Arbor, MI, USA.

He was a Visiting Professor with the Technical University of Munich, Munich, Germany, in 2002, a Visiting Professor with GTRI-Ireland, Athlone, Ireland, in 2009, and a Visiting Professor with LAAS-CNRS, Toulouse, France, in 2010. He has served as the Head of the GT-ECE Electromagnetics Technical Interest Group, as the Georgia Electronic Design Center Associate Director for RFID/Sensors Research, as the Georgia Tech NSF-Packaging Research Center Associate Director for RF Research, and as the RF Alliance Leader. He is currently the Ken Byers Professor of flexible electronics with the School of Electrical and Computer Engineering, Georgia Institute of Technology, Atlanta, GA, USA. He has authored over 620 papers in refereed journals and conference proceedings, 5 books, and 25 book chapters. He has helped develop academic programs in 3-D/inkjet-printed RF electronics and modules, flexible electronics, origami and morphing electromagnetics, highly integrated/multilayer packaging for RF and wireless applications using ceramic and organic flexible materials, paper-based RFID's and sensors, wireless sensors and biosensors, wearable electronics, Green electronics, energy harvesting and wireless power transfer, nanotechnology applications in RF, microwave MEMS, SOP-integrated UWB, multiband, mmW, conformal antennas and heads the Agile Technologies for High-Performance Electromagnetic Novel Applications Group (20 researchers).

Prof. Tentzeris is a member of URSI-Commission D, a member of MTT-15 Committee, an Associate Member of EuMA, a Fellow of the Electromagnetic Academy, and a member of the Technical Chamber of Greece. He served as one of the IEEE MTT-S Distinguished Microwave Lecturers from 2010 to 2012 and the IEEE CRFID Distinguished Lecturers. He was a recipient/co-recipient of the 2016 Bell Labs Award 3rd Prize, the 2015 IET Microwaves, Antennas and Propagation Premium Award, the 2014 Georgia Tech ECE Distinguished Faculty Achievement Award, the 2014 IEEE RFID-TA Best Student Paper Award, the 2013 IET Microwaves, Antennas and Propagation Premium Award, the 2012 FiDiPro Award in Finland, the iCMG Architecture Award of Excellence, the 2010 IEEE Antennas and Propagation Society Piergiorgio L. E. Uslenghi Letters Prize Paper Award, the 2011 International Workshop on Structural Health Monitoring Best Student Paper Award, the 2010 Georgia Tech Senior Faculty Outstanding Undergraduate Research Mentor Award, the 2009 IEEE TRANSACTIONS ON COMPONENTS AND PACKAGING TECHNOLOGIES Best Paper Award, the 2009 E. T. S. Walton Award from the Irish Science Foundation, the 2007 IEEE APS Symposium Best Student Paper Award, the 2007 IEEE IMS Third Best Student Paper Award, the 2007 ISAP 2007 Poster Presentation Award, the 2006 IEEE MTT-S Outstanding Young Engineer Award, the 2006 Asia–Pacific Microwave Conference Award, the 2004 IEEE TRANSACTIONS ON ADVANCED PACKAGING COMMENDABLE Paper Award, the 2003 NASA Godfrey Art Anzic Collaborative Distinguished Publication Award, the 2003 IBC International Educator of the Year Award, the 2003 IEEE CPMT Outstanding Young Engineer Award, the 2002 International Conference on Microwave and Millimeter-Wave Technology Best Paper Award, Beijing, China, the 2002 Georgia Tech-ECE Outstanding Junior Faculty Award, the 2001 ACES Conference Best Paper Award, the 2000 NSF CAREER Award, and the 1997 Best Paper Award of the International Hybrid Microelectronics and Packaging Society. He was the Technical Program Committee Chair at the IEEE IMS 2008 Symposium and the Chair of the 2005 IEEE CEM-TD Workshop. He is the Vice Chair of the RF Technical Committee (TC16) of the IEEE CPMT Society. He is the Founder and Chair of the RFID Technical Committee (TC24) of the IEEE MTT-S and the Secretary/Treasurer of the IEEE C-RFID. He is an Associate Editor of the IEEE TRANSACTIONS ON MICROWAVE THEORY AND TECHNIQUES, the IEEE TRANSACTIONS ON ADVANCED PACKAGING, and the *International Journal on Antennas and Propagation*. He has given over 100 invited talks to various universities and companies all over the world.